Effect of the active metal supported on SiO_2 to the selective hydrogen production on the glycerol steam reforming reaction

K.N. Papageridis[1,2], G. Siakavelas[1], N.D. Charisiou[1], M.A. Goula[1,2,*]

[1]Department of Environmental and Pollution Control Engineering, Technological Educational Institute of Western Macedonia (TEIWM), GR – 50100, Koila, Kozani, Greece

[2]Catalysis and Environmental Protection MSc, School of Science and Technology, Hellenic Open University, Parodos Aristotelous 18, GR - 26335, Patras, Greece

Keywords: hydrogen, glycerol, steam reforming, SiO_2 supported catalysts

Presenting author e-mail: mgoula@teiwm.gr

ABSTRACT

Climate change and the finite nature of fossil fuels have helped the development of biofuels as the only realistic alternative to petro-oil, with biodiesel experiencing an increase of almost 3000% in its production between 2000 and 2012, exceeding 430 thousand barrels per day. One of the more vocal advocates of biodiesel development has been the European Union, setting a target to deliver 10 per cent of energy in transport from renewable sources by 2020, and separately, to reduce the GHG lifecycle emissions of transport fuels by 6 per cent by 2020.

The principal byproduct of the biodiesel industry is glycerol, as every 10 g of oil undergoing the transesterification process produces 1 g of crude glycerol as byproduct, containing a number of impurities that prevent it from being used as raw material in the pharmaceutical and cosmetic industries. Hence, the excess of crude glycerol produced in the biodiesel industry (exceeding 2 million metric tons in 2012) is leading glycerol to be considered as a waste instead of a co-product. The production of hydrogen using glycerol as feedstock is one of the most interesting options, as hydrogen is considered a clean energy source whose demand is expected to greatly increase in the future, mainly due to technological advancements in the fuel cell industry.

Based on this background, a comparative study of catalytic performance for nickel (Ni), cobalt (Co) and copper (Cu) supported on silica catalysts, for the glycerol steam reforming reaction, is reported in this contribution. Catalysts were synthesized applying the incipient wetness impregnation method at a constant metal loading (5 wt. %). The synthesized samples were characterized by N_2 porosimetry (BET method) at their calcinated form and by XRD at calcinated and reduced forms. The chemical composition of the catalysts was determined by ICP, while the deposited carbon on the catalytic surface during the reaction was measured by a CHN analyzer. Catalysts' performance for glycerol steam reforming was studied in order to investigate the effect of the reaction temperature on (i) Glycerol total conversion, (ii) Glycerol conversion to gaseous products, (iii) Hydrogen selectivity and yield, (iv) Selectivity of gaseous products, and (v) Selectivity of liquid products. From the work presented herein, it can be concluded that Ni based on silica catalysts are more active and produce less liquid effluents than Co or Cu based on silica catalysts.

1. Introduction

Arguably, fossil fuels have helped built our current civilization, created our wealth and enriched the lives of billions. But they also have rising costs to our security, economy, health and environment that are starting to erode, if not outweigh their benefits. Recent statistical data from the World Energy Council shows that 82% of the total commercial energy consumed in the world was derived from fossil sources, with the figure being even higher in the transport sector, standing at 98% [1]. Serious concerns about the future availability of those non-renewable fuels, especially oil, have been prominent in public awareness and discourse since the oil crisis of the 1970's [e.g.; 2-4] However, increased anxiety is being caused by the ever growing emissions of manmade greenhouse gases (GHG), caused by the burning of fossil fuels, and the subsequent effects on the planet's climate and biodiversity.

Among the various Renewable Energy Systems (RES) that have been developed, the use of biomass as potential energy provider has gained considerable attention, especially in the field of biofuels, as the only realistic alternative to petro-oil [eg, 5,6]. Figure 1, depicts the world biofuel production from 2007 to 2012. As can be seen, bioethanol production, after reaching a peak in 2010 has experienced a gradual decrease in 2011 and 2012 [7]. Biodiesel production reached a peak in 2011 and stalled in 2012. However bioethanol production still remains more than triple that of biodiesel.
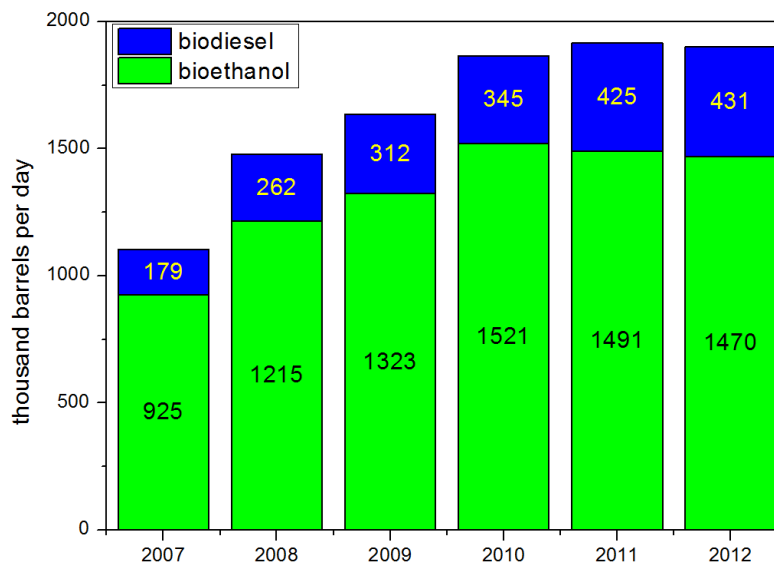
Figure 1. Total biofuels production (biodiesel and bioethanol) in the world in thousands of barrels per day from 2007-2012 [7]

Biodiesel is currently produced from the transesterification reaction between vegetable oils or animal fats (mainly, sunflower, rapeseed oils, palm oil, canola oil, cotton seed, soybean, Jatropha curcas, algae, waste frying oils, non-edible oils) and principally methanol (although ethanol is also used to a lesser extent) in the presence of an acidic or alkaline catalyst to form the biodiesel; fatty acid methyl esters (FAME) or fatty acid ethyl esters, as shown in Eq. 1 [8-10].

$$C_3H_5\left(OOC\right)_3\left(R_n\right)_3 + 3R'OH \;\rightleftharpoons\; 3R_nCOOR' + C_3H_5\left(OH\right)_3 \qquad\qquad (1)$$
$$\underset{Glycerides}{} \qquad\qquad \underset{Alcohols}{} \qquad\qquad \underset{Esters}{} \qquad \underset{Glycerol}{}$$
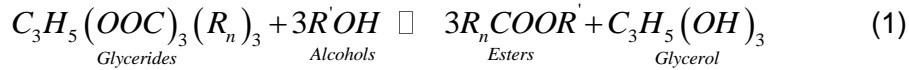
Figure 2 depicts the major biodiesel producing countries in the world. Interestingly, biodiesel production is not dominated by a handful of producers or a particular geographic region (as is the case with oil and natural gas); rather a number of countries have been developing this resource. Although not shown on Figure 2, additional countries such as India, Malaysia, the Philippines, Colombia and Canada have also been notable in increasing biodiesel production.
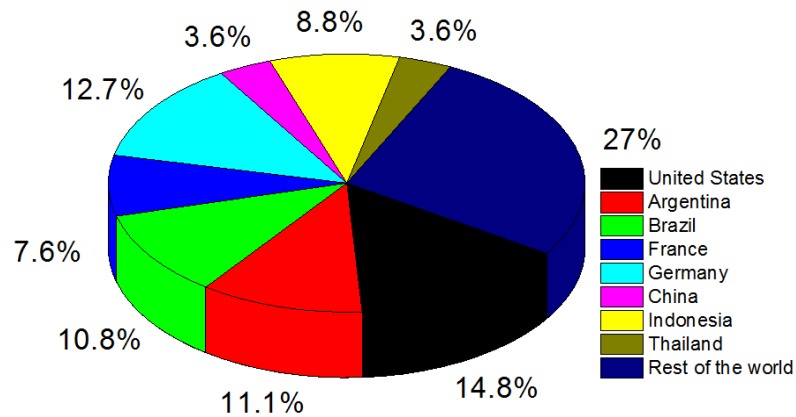
Figure 2. Major biodiesel producers (%) in 2012 [7]

Over the past decade, biodiesel has moved from being a niche energy source in the European transport sector to being a significant source of road transport fuel, with the EU 27 experiencing an increase in the use of biodisel of over 70% between 2007 and 2012 [7]. Germany and France have mainly bore the brunt of this increase, with Italy, Spain, Austria, Belgium, Netherlands, Portugal and Poland being the next notable producers (Fig. 3). At present, the EU has a target to deliver 10 per cent of energy in transport from renewable sources by 2020, and separately, to reduce the GHG lifecycle emissions of transport fuels by 6 per cent by 2020 [11,12]. Naturally, the pursuit of these twin targets promotes the expansion of biofuels, and mainly that of biodiesel, as bioethanol production in the EU is minimal.

However, since 2012, there has been an intense debate as to how best to address current failings in the policy mechanisms underpinning EU support. This has largely focused on how to ensure that GHG accounting takes proper consideration of the emissions from indirect land use change (ILUC) associated with biofuel feedstock production. There is also recognition that EU policy has led to the adoption of predominantly conventional biofuels, i.e. those using primarily food or feed-based feedstocks reliant on land for their production. Moreover, technological and logistical advances towards biofuels using non landbased feedstocks such as waste and residues have only materialised slowly. These issues are yet to be resolved, with proposed amendments to the relevant legislation currently stalled [13, 14].

In any case, one of the barriers for the further development and commercialization of biodiesel is its high production cost, which is caused by the price of raw materials [15,16]. Thus, the industry needs to find new and innovative ways of maximizing its profits either by bringing down

the cost of raw materials (hence the move towards making use of waste cooking oils) and/or by making use of its existing waste streams.
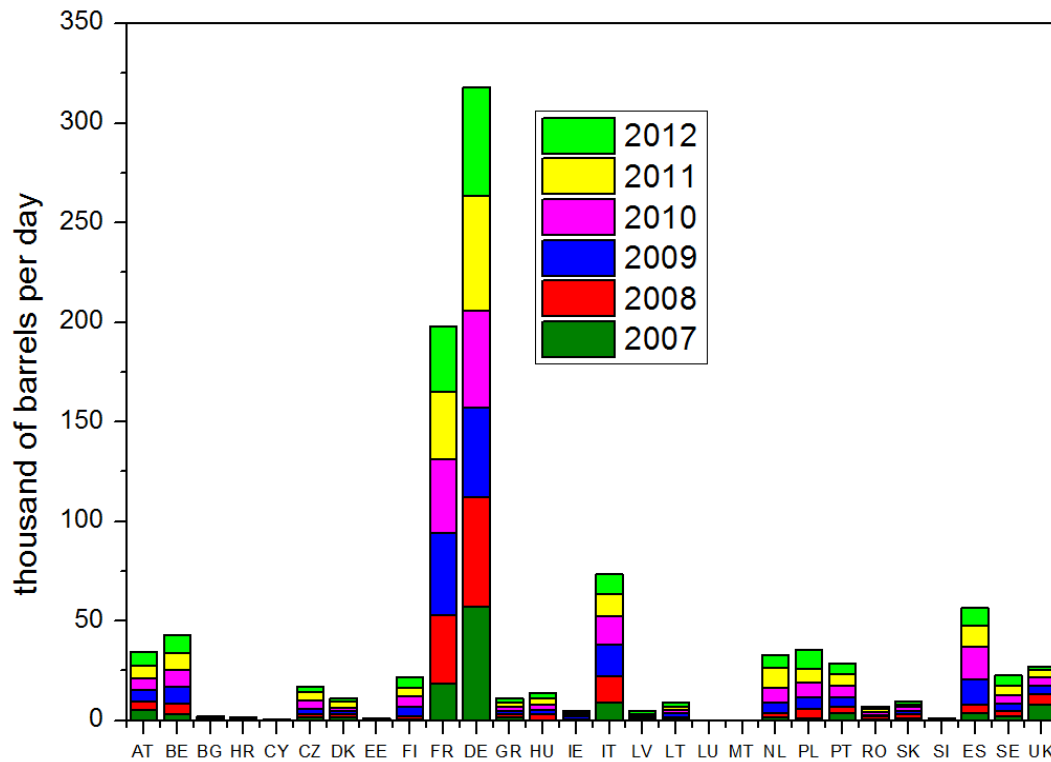
Figure 3. EU-27 biodiesel production in thousand of barrels per day from 2007-2012 [7]

The principal byproduct of the biodiesel industry is glycerol, as every 100g of oil undergoing the transesterification process produces 10g of glycerol as byproduct. The glycerol so obtained is crude as it contains non-reacted and partially reacted fats, free fatty acids, methanol, esters and salts, and thus, it cannot be used as raw material in the pharmaceutical and cosmetic industries [17]. A viable solution could be the reconstruction of biodiesel plants into novel biorefineries through the integration of glycerol-based bioconversions in existing lines for the production of various chemicals [18] or the production of synthesis gas and hydrogen [19]. Moreover, it is important to note that the excess of crude glycerol produced (Fig. 4) in the biodiesel industry (exceeding 2 million metric tons in 2012) is leading to a decrease in glycerol prices, with glycerol now being considered as a waste instead of a co-product [20].

The production of hydrogen is one of the most interesting options, as hydrogen is considered a clean energy source and has numerous uses. Moreover, the demand for hydrogen is expected to greatly increase in the future, mainly due to technological advancements in the fuel cell industry [21,22]. At present, almost half of the hydrogen produced worldwide is generated through the steam reforming of methane (SRM), with the reforming of naphtha/oil accounting for 30%, coal gasification for 18% and electrolysis for only 4% [23]. Hydrogen can be produced from glycerol by catalytic steam reforming (SR) [e.g. 24-28], oxidative steam reforming [29], autothermal reforming (ATR) [30,31], aqueous phase reforming (APR) [32-35], and supercritical

water (SCW) reforming [36-38]. However, the reaction that has attracted most attention is that of the steam reforming, partially due to the fact that the process is widely used in industry, and would require only minor alterations in existing systems if the feedstock was changed from natural gas or naphtha to glycerol [23].
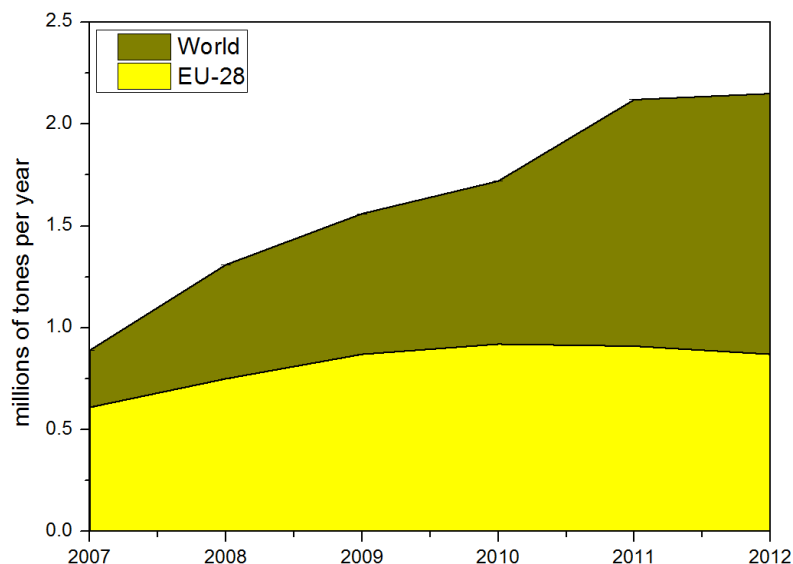
Figure 4. World and EU-28 glycerol production in millions of tones per year from 2007-2012 (calculations based on an average biodiesel density of 0.86 g/cm^3)

Based on this background, a comparative study of catalytic performance for nickel (Ni), cobalt (Co) and copper (Cu) supported on silica catalysts, for the glycerol steam reforming reaction, is reported in this contribution. Catalysts were synthesized applying the incipient wetness impregnation method at a constant metal loading (5 wt. %). The synthesized samples were characterized by N_2 porosimetry (BET method) at their calcinated form and by XRD at their calcinated and reduced forms. The chemical composition of the catalysts was determined by ICP, while the deposited carbon on the catalytic surface during the reaction was measured by a CHN analyzer. Catalysts' performance for glycerol steam reforming was studied in order to investigate the effect of the reaction temperature on (i) Glycerol total conversion, (ii) Glycerol conversion to gaseous products, (iii) Hydrogen selectivity and yield, (iv) Selectivity of gaseous products, and (v) Selectivity of liquid products.

2. Experimental

2.1 Catalysts preparation and characterization
The silica support, which was obtained from Englelhard (SDS code: SI-1624E) in powder form, was first pelletized and then crashed and sieved to 350-500μm, before being calcined at 800 $^{\circ}$C for 4 h. The catalysts were prepared via the incipient wetness impregnation method, by impregnating the SiO_2 with $Ni(NO_3)_2$ $6H_2O$, $CO(NO_3)_2$ $6H_2O$ and $Cu(NO_3)_2$ $6H_2O$, aqueous solutions having the appropriate concentration, in order to obtain 5 wt. % Ni, Co and Cu

respectively in the final catalysts (the catalysts were labeled as Ni/Si, Co/Si and Cu/Si). The total volume of the impregnation solutions was equal with the total pore volume of the silica used. The impregnated samples were dried overnight and calcined at 800 ^{o}C for 5 hours. All solutions for the catalysts preparation utilized distilled and deionised pure water generated by NANOpure Diamond UV unit (Barnstead International).

Surface areas (S_{BET}) of the catalytic samples were determined by the N_2 adsorption–desorption isotherms at -196°C using the Nova 2200e (Quantachrome) flow apparatus, according to Brunauer-Emmett-Teller (BET) method at the relative pressure in the range of 0.05–0.30. The total pore volume calculation was based on nitrogen volume at the highest relative pressure, whereas the average pore size diameter was determined by the Barrett-Joyner-Halenda (BJH) method. Prior to the measurements the samples were degassed at 350 ^{o}C for 5 h under vacuum.

The total metal loading (wt. %) of the final catalysts was determined by Inductively Coupled Plasma Atomic Emission Spectroscopy (ICP-AES) on a Perkin-Elmer Optima 4300DV apparatus. The wavelengths selected were at 341.476, 227.022, and 231.604 nm. The selected conditions of the measurement were: Plasma flow: 15 L/min, Auxiliary flow: 0.2 L/min, Nebulize flow: 0.6 L/min, RF Power: 1300 watts, Plasma View: radial view, and Sample Flow Rate: 2 mL/min. The acid digestion procedure involved the weighting of each sample to the nearest 0.00001 g in a Teflon beaker and its transportation to a fume hood, where 1 ml of concentrated sulphuric acid was added. The mixture was then heated to dryness at low heat on a hot plate overnight. Afterwards, 2 ml of concentrated hydrochloric acid and 2 ml of concentrated nitric acid were added to the beaker with the heating being terminated after 5-10 min, when the reaction of dissolution was completed. At this point, about 2 ml of de-ionized water were added and the beaker was left to cool. The resulting clear solution was loaded carefully in a 50 ml volumetric flask in order to make up an accurate fixed volume adding de-ionized water. Each sample was measured thrice, in order to check repeatability.

The catalysts' crystalline structure was determined by applying the X-ray diffraction (XRD) technique, using a ThermoAl diffractometer at 40 kV and 30 mA with Cu K_{α} radiation (λ=1.54178 nm). Diffractograms were recorded in the 2θ=2-70 range at a scanning rate of 0.04 over 1.2 min^{-1}. The diffraction pattern was identified by comparison with those of known structure in the JCPDS (Joint Committee of Powder Diffraction Standards) database. It should be noted that the XRD technique was used for both fresh and reduced samples.

The percentile concentration of carbon in the used catalysts was measured by quantitative infrared spectroscopy performed with a Leco CHN-200 analyser, using 0.1 g of each sample.

2.2 Catalytic performance
The glycerol steam reforming reaction was carried out at atmospheric pressure, in a continuous flow, fixed-bed, single pass, tubular stainless steel reactor, with an inner diameter of 14 mm, at temperature ranging from 400-750 ^{o}C (Fig. 5). The experimental set up used allowed the feeding of both liquid and gaseous streams, having two vaporizers and a pre-heater before the reactor and a condenser after it. The vaporizers, pre-heater and reactor are placed into electrical ovens and regulated with programmed-temperature controllers.

The liquid stream consisted of $C_3H_8O_3$ (20% w.w.) and H_2O (total liquid flow rate = 0.12 ml/min). The glycerol used had 99.5% purity and was obtained from Sigma Aldrich. The glycerol/ water

mixture was fed with a HPLC pump (Series I) and was first vaporized at 350°C before it was mixed with He (He flow rate = 38 ml/min). The reactor's outlet gases passed through a cold trap for liquid products capture. Prior to catalytic testing, 200 mg of catalyst was reduced in situ in a hydrogen flow (100 ml/min) at 800 °C for 1 hr. The gaseous products were analyzed on-line by a gas chromatographer (Agilent 7890A), with two columns in parallel, HP-Plot-Q (19095-Q04, 30 m length, 0.530 mm I.D.) and HP-Molesieve (19095P-MSO, 30 m length, 0.530 mm I.D.), equipped with TCD and FID detectors. Liquid products were analyzed via a combination of Gas Chromatography (Agilent 7890A, with a 5MS column, equipped with an FID detector) and Mass Spectroscopy (Agilent 5975C).
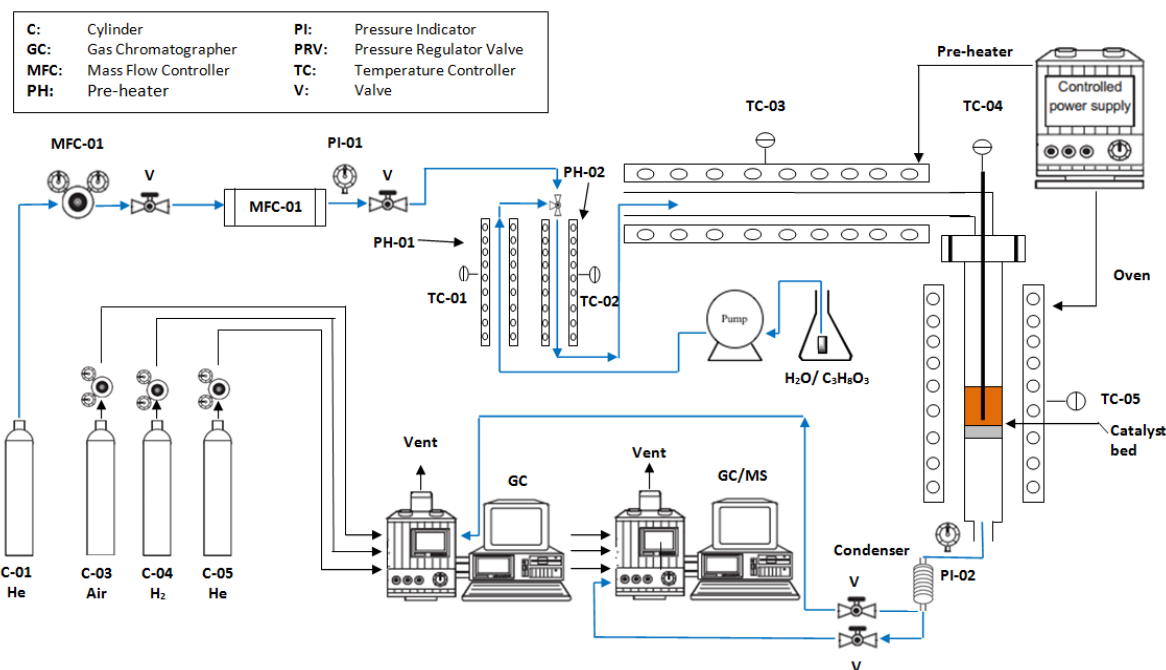
Figure 5. Schematic flow chart of experimental setup for activity test of catalysts towards glycerol steam reforming

Catalytic performance is reported in terms of H_2 yield, H_2, CO, CH_4 and CO_2 selectivity, glycerol conversion into gaseous products, and total glycerol conversion (global conversion). Moreover, the performance of the catalysts in the liquid phase is reported in terms of acetol ($C_3H_6O_2$), acetone [$(CH_3)_2CO$], allyl alcohol ($CH_2=CHCH_2OH$), acetaldehyde (C_2H_4O) and acetic acid (C_2H_4O) selectivity. Performance parameters were calculated based on the following equations:

$$\% \, glycerol \, conversion_{(global \, conversion)} = \left(\frac{Glycerol_{in} - Glycerol_{out}}{Glycerol_{in}} \right) \times 100 \tag{2}$$

$$\% \, glycerol \, conversion_{(gaseous \, products)} = \left(\frac{C \, atoms \, in \, the \, gas \, products}{total \, C \, atoms \, in \, the \, feedstock} \right) \times 100 \tag{3}$$

$$H_2 \ yield = \frac{H_2 \ moles \ produced}{moles \ of \ glycerol \ in \ the \ feedstock} \qquad (4)$$

$$\% H_2 \ selectivity = \left(\frac{H_2 \ moles \ produced}{C \ atoms \ produced \ in \ the \ gas \ phase}\right) \times \left(\frac{1}{RR}\right) \times 100 \qquad (5)$$

where, RR is the reforming ratio (7/3), defined as the ratio of moles of H_2 to CO_2 formed.

$$\% \ selectivity \ of \ i = \left(\frac{C \ atoms \ in \ species \ i}{C \ atoms \ produced \ in \ the \ gas \ phase}\right) \times 100 \qquad (6)$$

where, species i refers to CO, CO_2 and CH_4.

$$\% \ selectivity \ of \ i' = \left(\frac{C \ atoms \ in \ species \ i'}{C \ atoms \ produced \ in \ the \ liquid \ phase}\right) \times 100 \qquad (7)$$

where, species i' refers to acetol, acetone, allyl alcohol, acetaldehyde and acetic acid.

3. Results and discussion

3.1 Characterisation results

In Table 1 the physicochemical properties of all samples are presented. As can be observed, the specific surface area (SSA, i.e., S_{BET}) and the pore volume (Vp) for all catalysts is lower than the one of the supporting material. The lower surface area can be attributed to the fact that the internal surface area of the support pore system is probably progressively covered by nickel, cobalt and copper species adsorbed on silica's active sites forming a layer [39]. Nonetheless, it is worth pointing out that all three samples have comparable SSA and Vp to one another. Moreover, the ICP results (metal loading) indicate that the desired metal levels were achieved for all samples.

Table 1. Physicochemical properties of the calcinated samples

Sample	S_{BET} (m^2g^{-1})	V_p $(ml \ g^{-1})$	Metal loading ICP (wt%)
SiO_2	108.27	0.86	-
Ni/Si	84.09	0.69	4.86
Co/Si	87.01	0.74	4.73
Cu/Si	71.92	0.64	4.85

Figure 6 depicts the XRD patterns of the Ni/SiO_2 catalyst after calcination and after reduction. Characteristic peaks at $2\theta=21.9^{o}$, corresponding to SiO_2 (Cristobalite) and $2\theta=26.5^{o}$ corresponding to SiO_2 (Quartz) are observed for both samples. The nickel oxide (NiO) structure was detected at $2\theta=37.2^{o}$ and 43.2^{o} on the calcined sample, while on the reduced sample we observed the appearance of two small peaks due to the presence of metallic nickel (Ni^0) at

$2\theta=44.3^o$ and 51.7^o. Figure 7 depicts the XRD patterns of the Co/SiO_2 and Cu/CiO_2 catalyst after reduction. SiO_2 (Cristobalite) and SiO_2 (Quartz) where observed for both catalysts at the same 2θ as above. Metallic cobalt (Co^0) was detected at $2\theta=44.05^o$ and 51.4^o for the Co/Si sample, and metallic Cu (Cu^0) at $2\theta=43.24^o$ and 50.36^o for the Cu/Al sample. The crystalline phases that were detected for the SiO_2 support and for the catalysts in their calcinated and reduced forms are summarized in Table 2.
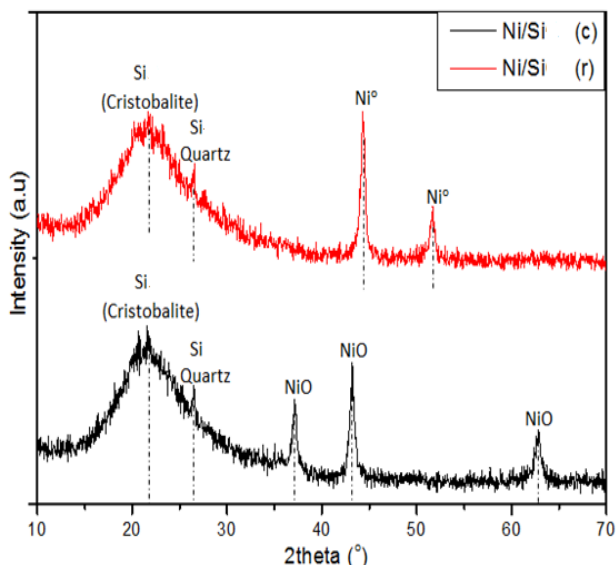
Figure 6. XRD patterns of calcined and reduced (at 800^oC) Ni/Si catalysts
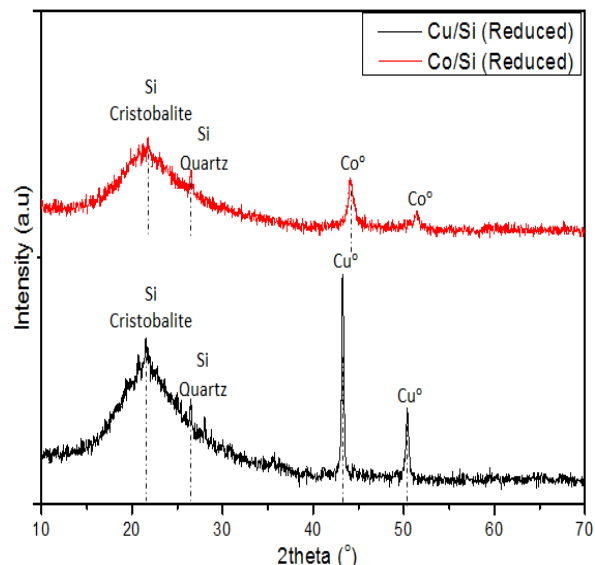
Figure 7 XRD patterns of reduced (at 800^oC) Co/Si and Cu/Si catalysts

Table 2. Crystalline phases of support and catalysts

Sample	Crystalline phases
SiO_2 (c)	SiO_2 (Cristobalite), SiO_2 (Quartz)
Ni/Si (c)	SiO_2 (Cristobalite), SiO_2 (Quartz), NiO
Ni/Si (r)	SiO_2 (Cristobalite), SiO_2 (Quartz), Ni
Co/Si(c)	SiO_2 (Cristobalite), SiO_2 (Quartz), Co_3O_4, Co_2SiO_4
Co/Si (r)	SiO_2 (Cristobalite), SiO_2 (Quartz), Co
Cu/Si (c)	SiO_2 (Cristobalite), SiO_2 (Quartz), CuO
Co/Si (r)	SiO_2 (Cristobalite), SiO_2 (Quartz), Cu

Note: c=calcinated, r=reduced

3.2. Catalytic activity and selectivity

Thermodynamic studies predict that high temperatures, low pressures and high H_2O/C ratio favor hydrogen production. A number of researchers suggest that the ideal condition to obtain hydrogen is at reaction temperatures between 627 and 700 ^oC, with a molar ratio of water to glycerol higher than 9. Under these conditions, methane production is minimized and carbon formation is thermodynamically inhibited. Although excess water allows higher selectivity to hydrogen, a significant water amount in reaction products is not beneficial [24,25,40-43]. Thus,

in this work, reaction tests were carried out in a temperature range of 400-750 ^{o}C, at atmospheric pressure and for a water-glycerol molar ratio of 20:1.
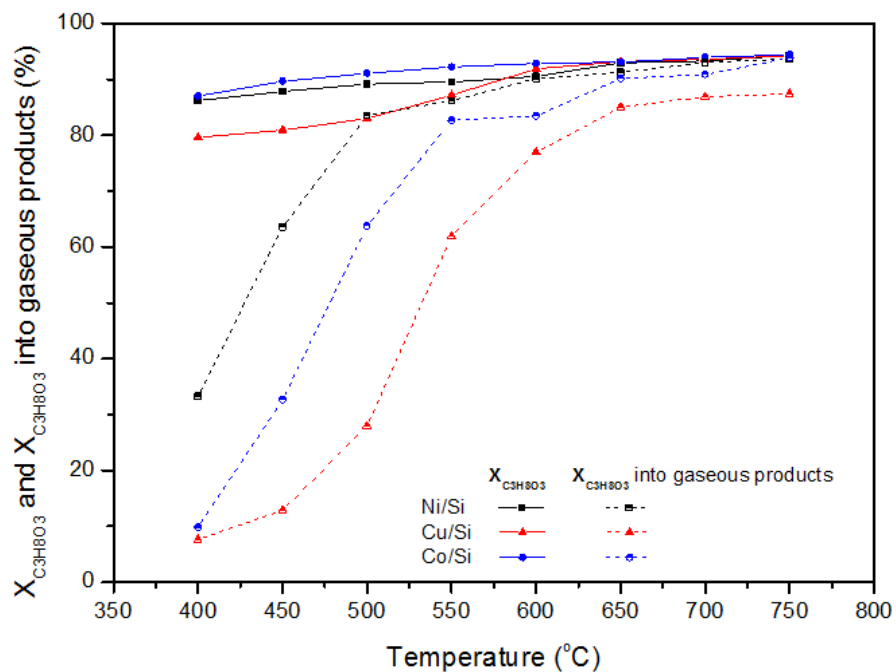
Figure 8. Total glycerol conversion and glycerol conversion into gaseous products for the Ni/Si, Cu/Si and Co/Si catalysts
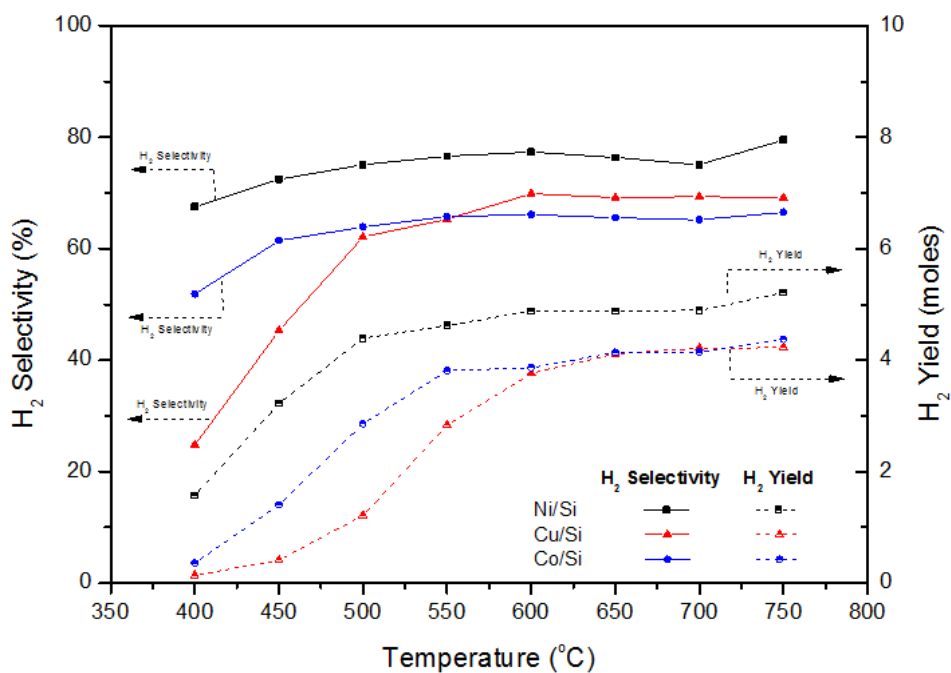
Figure 9. Hydrogen yield and selectivity for the Ni/Si, Cu/Si and Co/Si catalysts

Glycerol total conversion and glycerol conversion into gaseous products is presented in Figure 8. As can be clearly observed, all three catalysts show improvements with increased temperatures, which is a consequence of the endothermic nature of the overall steam reforming reaction; however, the Ni/Si catalyst exhibits significantly higher conversions into gaseous products. In fact, as can be observed from Figure 8, the sequence of catalytic performance is Ni/Si>Co/Si>Cu/Si. Glycerol total conversion is essentially flat for all the catalysts, with the Cu/Si sample performing the worse. It should be noted that this high glycerol total conversion has been observed by all researchers concerned with this reaction [e.g. 26,44].
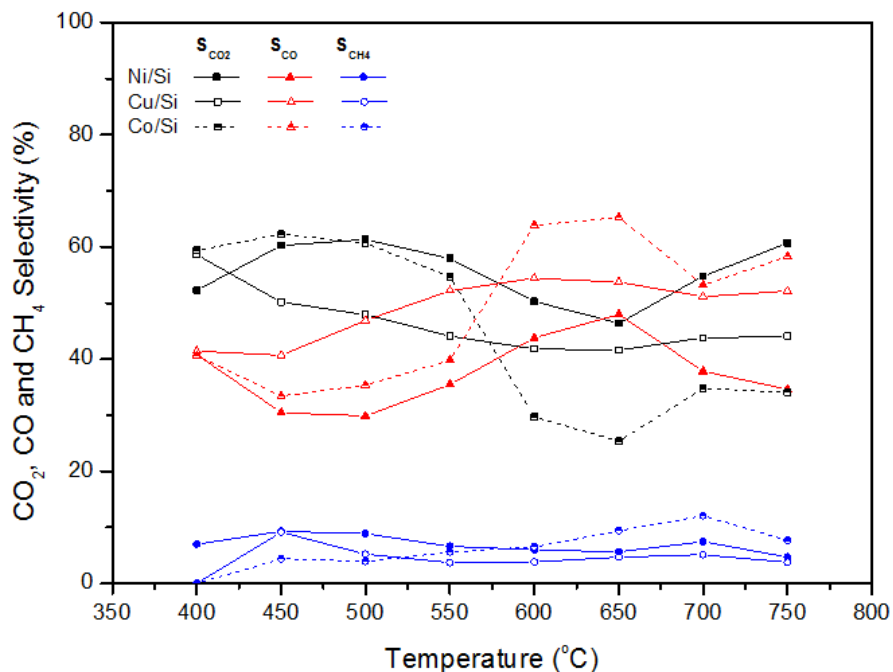
Figure 10. CO_2, CO and CH_4 selectivity for the Ni/Si, Cu/Si and Co/Si catalysts

The GC analysis revealed that the gaseous products were H_2, CO_2, CO and CH_4, which is in line with previous work by other researchers that have also indicated that above reaction temperatures of 400 ^oC these gases are the major products of glycerol steam reforming [45-49]. Hydrogen yield and selectivity (%) are presented in Figure 9. Hydrogen selectivity increases with increasing temperatures for all catalysts however, their behavior is not similar to one another. The selectivity for the Cu/Si sample begins at low values (≈25%) at 400 ^oC, and increases sharply up to 500 ^oC; from then on it almost plateaus. On the contrary, for both Ni/Si and Co/Si samples, hydrogen selectivity has high initial values (≈70% and ≈50% respectively), but the increase is very gradual, also almost terminating at 500 ^oC. The sequence of catalytic performance, in terms of H_2 yield (moles), is again Ni/Si>Co/Si>Cu/Si (Fig. 9). It is noteworthy however that although the Co/Si sample exhibits higher hydrogen yield than the Cu/Si sample between 400-600 ^oC, above this temperature the two catalysts have similar selectivity's.

The selectivity of CO_2, CO and CH_4 for all three catalysts is presented in Figure 10. For all three catalysts, the formation of CH_4 is considerably low during the whole test, which can be attributed to the steam reforming of methane derived from glycerol decomposition [28]. For the Ni/Si

sample, CO_2 selectivity decreases up to 650 ^{o}C and then it experiences a relatively sharp increase; the opposite is true for CO selectivity, i.e., it increases up to 650 ^{o}C, before decreasing. For the Co/Si catalyst, carbon monoxide and carbon dioxide selectivity exhibit a volcano and reverse volcano type behavior, between 550-700 ^{o}C. The CO_2 selectivity for the Cu/Si sample has a very slight downward slope during reaction, while CO selectivity a gradual upward trajectory. It is noted that the presence of CO in the gas mixture is significant, as it can adversely affect the performance of both anode and cathode in proton-exchange fuel cells (PEMFCs) acting as poison [50,51].
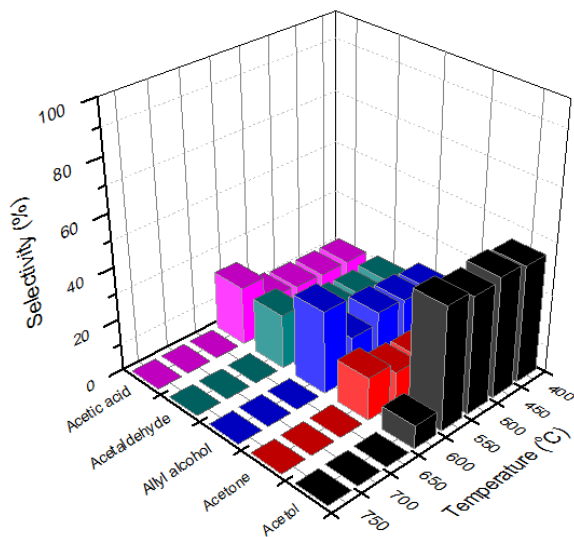
Figure 11. Liquid products' selectivity for the Ni/Si catalyst
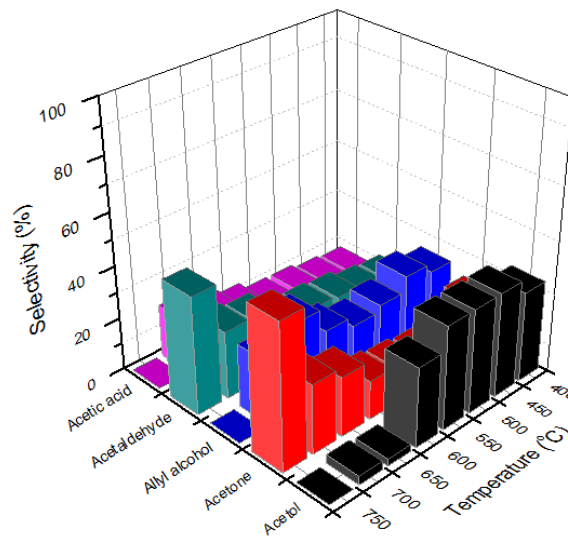
Figure 12. Liquid products' selectivity for the Cu/Si catalyst
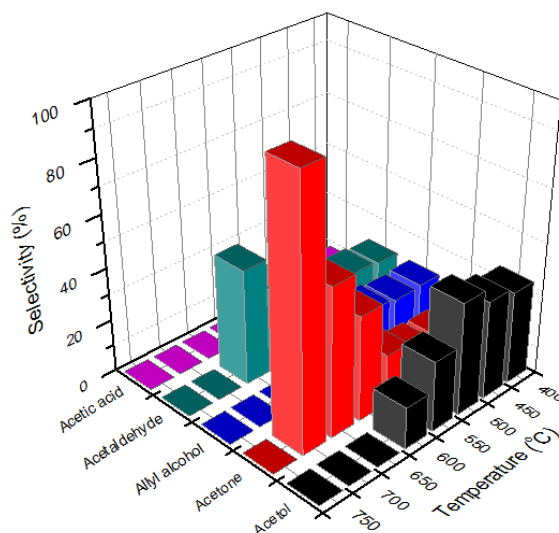
Figure 13. Liquid products' selectivity for the Co/Si catalyst

Condensed reaction products (liquid products) presented a yellowish colour and by combined gas chromatography and mass spectroscopy (CG/MS), a number of compounds were identified

and quantified. The compounds identified for all three catalysts were acetic acid, acetaldehyde, allyl alcohol, acetone and acetol. For the Ni/Si catalyst these products where present mainly at relatively low temperature ranges, i.e., from 400 – 600 ^{o}C (Fig. 11), which can be attributed to the different reaction routes that convert glycerol to liquid products (e.g. glycerol hydrogenolysis) that are exothermic in character [41]. However, for both the Cu/Si and Co/Si samples (Figs. 12 and 13 respectively), liquid effluents were produced throughout the catalytic testing (i.e., from 400 – 750 ^{o}C).

Table 3. Carbon concentration in the used catalysts

Sample	Carbon (%)
Ni/Si	23.62
Co/Si	9.97
Cu/Si	12.65

Unfortunately, studies on carbon deposition over Ni-based catalysts and the mechanism of coke formation for the steam reforming of glycerol are still missing in the literature. However, some contributions have reported the deactivation of Ni-supported catalysts on SR of glycerol and associated this phenomenon with the formation of both highly reactive carbon species and low reactive, more ordered structures, particularly filamentous carbon [25,26,41,48,52]. This can probably provide an explanation for the results depicted on Table 3, of the percentile concentration of carbon as measured on the used catalysts, where despite the fact the Ni/Si catalyst exhibits a better catalytic performance that the other two samples, more carbon has been deposited on its surface.

4. Conclusions

The need to move from fossil based resources in the transport sector led to the promotion of biofuels as the only realistic alternative to petro-oil. However, the increase in biodiesel production has been accompanied by increases in glycerol production, which is the main by-product of the process. As the production of glycerol exceeded 2 million metric tons in 2012, it is now considered as a waste instead of a co-product. Arguably, glycerol valorization to hydrogen is one of the prospective ways to alleviate our dependence on fossil fuels and mitigate this waste management issue with heterogeneous catalysis playing a critical role in converting glycerol to a valuable product.

From the work presented herein, it can be concluded that Ni based on silica catalysts are more active and produce less liquid effluents than Co or Cu based on silica catalysts.

REFERENCES

[1]   World Energy Council 2013, https://www.worldenergy.org/data/resources/ (*accessed at 30/5/2015*).

[2]   Almeida, P., Silva, P.D., 2009. The peak of oil production: Timings and market recognition. Energy Policy 37, 1267-1276.

[3]   Bentley, R.W., 2002. Global oil & gas depletion: an overview. Energy Policy 30, 189–205.

[4]   Jakobsson, K., Bentley, R., Soderbergh, B., Aleklett, K., 2012. The end of cheap oil: Bottom-up economic and geologic modeling of aggregate oil production curves. Energy Policy 41, 860–870.

[5]   Panepinto, D., Viggiano, F., Genon, G., 2014. Evaluation of environmental compatibility for a biomass plant. Waste and Biomass Valorization, 5(5), 759-772.

[6]   Yeon, S.H., Shin, D.H., Nho, N.S., Shin, K.H., Jin, C.S., 2013. Economic feasibility of ethanol production from biomass and waste resources via catalytic reaction. Waste Management & Research, 31(4), 421-427.

[7]   US Energy Information Administration (EIA), International Energy statistics, http://www.eia.gov/cfapps/ipdbproject/IEDIndex3.cfm (*accessed at 30/5/2015*).

[8]   Atadashi, I.M., Aroua, M.K., Abdul Aziz, A.R., Sulaiman, N.M.N., 2013. The effects of catalysts in biodiesel production: A review. Journal of Industrial and Engineering Chemistry, 19, 14-26.

[9]   Atapour, M., Kariminia, H.R., 2013. Optimization of biodiesel production from Iranian bitter almond oil using statistical approach. Waste and Biomass Valorization, 4(3), 467-474.

[10] Marx, S., Venter, R. 2014. Evaluation of waste process grease as feedstock for biodiesel production. Waste and Biomass Valorization, 5(1), 75-86.

[11] Murphy, F., Devlin, G., Deverell, R., McDonnell, K., 2014. Potential to increase indigenous biodiesel production to help meet 2020 targets – An EU perspective with a focus on Ireland. Renewable and Sustainable Energy Reviews, 35, 154-170.

[12] Yunus khan, T.M., Atabani, A.E., Badruddina, I.A., Badarudina, A., Khayoon, M.S., Triwahyono, S., 2014. Recent scenario and technologies to utilize non-edible oils for biodiesel production. Renewable and Sustainable Energy Reviews, 37, 840-851.

[13] Rincón, L.E., Jaramillo, J.J., Cardona, C.A., 2014. Comparison of feedstocks and technologies for biodiesel production: An environmental and techno-economic evaluation. Renewable and Sustainable Energy Reviews, 69, 479-487.

[14] Borugadda, V.B., Goud, V.V., 2012. Biodiesel production from renewable feedstocks: Status and opportunities. Renewable and Sustainable Energy Reviews, 16(7), 4763-4784.

[15] Nuchdang, S., Phalakornkule, C., 2012. Anaerobic digestion of glycerol and co-digestion of glycerol and pig manure. Journal of Environmental Management, 101, 164-172.

[16] Shin, H.Y., Ryu, J.H., Bae, S.Y., Kim, Y.C., 2013. Biodiesel production from highly unsaturated feedstock via simultaneous transesterification and partial hydrogenation in supercritical methanol. The Journal of Supercritical Fluids, 82, 251-255.

[17] Khanna, S., Shukla, A.K., Goyal, A., Moholkar, V.S., 2014. Alcoholic biofuels production from biodiesel derived glycerol by clostridium pasteurianum whole cells immobilized on silica. Waste and Biomass Valorization, 5(5), 789-798.

[18] Kachrimanidou, V., Kopsahelis, N., Chatzifragkou, A., Papanikolaou, S., Yanniotis, S., Kookos, I., Koutinas, A.A., 2013. Utilisation of by-products from sunflower-based biodiesel

production processes for the production of fermentation feedstock. Waste and Biomass Valorization, 4(3), 529-537.

[19] Escribà, M., Eras, J., Villorbina, G., Balcells, M., Blanch, C., Barniol, N., Canela R., 2011. Use of crude glycerol from biodiesel producers and fatty materials to prepare allyl esters. Waste and Biomass Valorization, 2(3), 285-290.

[20] Almeida, J.R.M., Fávaro, L.C.l., Quirino, B.F., 2012. Biodiesel biorefinery: opportunities and challenges for microbial production of fuels and chemicals from glycerol waste. Biotechnology for Biofuels, 5:48.

[21] Amoretti, M., 2011. Towards a peer-to-peer hydrogen economy framework. International Journal of Hydrogen Energy, 36, 6376-6386.

[22] Pudukudy,M., Yaakob, Z., Mohammad, M., Narayanan, B., Sopian, K., 2015. Renewable hydrogen economy in Asia–Opportunities and challenges: An overview. Renewable and Sustainable Energy Reviwes, 30, 743-757.

[23] Silva, J.M., Soria, M.A., Madeira, L.M., 2015. Challenges and strategies for optimization of glycerol steam reforming process. Renewable and Sustainable Energy Reviews, 42 1187-1213.

[24] Adhikari, S., Fernando, S., Haryanto, A., 2007. Production of hydrogen by steam reforming of glycerin over alumina-supported metal catalysts. Catalysis Today, 129, 355-364.

[25] Buffoni, I.N., Pompeo, F., Santori, G.F., Nichio, N.N., 2009. Nickel catalysts applied in steam reforming of glycerol for hydrogen production. Catalysis Communications, 10, 1656-1660.

[26] Cheng, C.K. Foo, S.Y., Adesina, A.A., 2011. Steam reforming of glycerol over Ni/Al_2O_3 catalyst. Catalysis Today, 178, 25-33.

[27] Iriondo, A., Barrio, V.L., Cambra, J.F., Arias, P.L., Güemez, M.B., Navarro, R.M., Sanchez-Sanchez M.C., Fierro, J.L.G., 2009. Influence of La_2O_3 modified support and Ni and Pt active phases on glycerol steam reforming to produce hydrogen. Catalysis Communications, 10(8), 1275-1278.

[28] Wang, C., Dou, B., Chen, C., Song, Y., Xu, Y., Du, X., Zhang, L., Luo, T., Tan, C., 2013. Renewable hydrogen production from steam reforming of glycerol by Ni-Cu-Al, Ni-Cu-Mg, Ni-Mg catalysts. International Journal of Hydrogen Energy, 38, 3562-3571.

[29] Alvarado, F.D., Gracia, F., 2012. Oxidative steam reforming of glycerol for hydrogen production: Thermodynamic analysis including different carbon deposits representation and CO_2 adsorption. International Journal of Hydrogen Energy, 37, 14820-14830.

[30] Dauenhauer, P.J., Salge, J.R., Schmidt, L.D., 2006. Renewable hydrogen by autothermal steam reforming of volatile carbohydrates. Journal of Catalysis, 244(2), 238-247.

[31] Wang, H., Wang, X., Li, M., Li, S., Wang, S., Ma, X., 2009. Thermodynamic analysis of hydrogen production from glycerol autothermal reforming. International Journal of Hydrogen Energy, 34(14), 5683-5690.

[32] Cortright, R.D., Davda, R.R., Dumesic, J.A., 2002. Hydrogen from catalytic reforming of biomass-derived hydrocarbons in liquid water. Nature, 418, 964-967.

[33] Manfro, R.L., da Costa, A.F., Ribeiro, N.F.P., Souza, M.M.V.M., 2011. Hydrogen production by aqueous-phase reforming of glycerol over nickel catalysts supported on CeO_2. Fuel Processing Technology, 92, 330-335.

[34] Menezes, A.O., Rodrigues, M.T., Zimmaro, A., Borges, L.E.P., Fraga, M.A., 2011. Production of renewable hydrogen from aqueous-phase reforming of glycerol over Pt catalysts supported on different oxides. Renewable Energy, 36(2), 595-599.

[35] Tuza, P.V., Manfro, R.L., Ribeiro, N.F.P., Souza M.M.V.M., 2013. Production of renewable hydrogen by aqueous-phase reforming of glycerol over Ni-Cu catalysts derived from hydrotalcite precursors. Renewable Energy, 50, 408-414.

[36] Byrd, A.J., Pant, K.K., Gupta, R.B. 2008. Hydrogen production from glycerol by reforming in supercritical water over Ru/Al_2O_3 catalyst. Fuel, 87, 2956–2960.

[37] Gutiérrez Ortiz, F.J., Serrera, A., Galera, S., Ollero, P., 2013. Experimental study of the supercritical water reforming of glycerol without the addition of a catalyst. Energy, 56,193-206.

[38] Pairojpiriyakul, T., Croiset, E., Kiatkittipong, W., Kiatkittipong, K., Arpornwichanop, A., Assabumrungrat, S., 2013. Hydrogen production from catalytic supercritical water reforming of glycerol with cobalt-based catalysts. International Journal of Hydrogen Energy, 38, 4368-4379.

[39] Bereketidou, O.A., Goula, M.A., 2012. Biogas reforming for syngas production over nickel supported on ceria-alumina catalysts. Catalysis Today 195, 93-100.

[40] Wang, X.D., Li, S.R., Wang, H., Liu, B., Ma, X.B., 2008. Thermodynamic analysis of glycerin steam reforming. Energy and Fuels, 22, 4285-4291.

[41] Franchini, C.A., Aranzaez, W., de Farias, A.M.D., Pecchi, G., Fraga, M.A., 2014. Ce-substituted $LaNiO_3$ mixed oxides as catalyst precursors for glycerol steam reforming. Applied Catalysis B: Environmental, 147, 193-202.

[42] Sad, M.E., Duarte, H.A., Vignatti, C.H., Padro, C.L., Apesteguıa, C.R., 2015. Steam reforming of glycerol: Hydrogen production optimization. International Journal of Hydrogen Energy, 40, 6097-6106.

[43] Freitas, A.C.D., Guirardello, R., 2014. Comparison of several glycerol reforming methods for hydrogen and syngas production using Gibbs energy minimization. International Journal of Hydrogen Energy, 39, 17969-17984.

[44] Ebshish, A., Yaakob, Z., Narayanan, B., Bshish, A., Daud, W.R.W., 2012. Steam Reforming of Glycerol over Ni Supported Alumina Xerogel for Hydrogen Production. Energy Procedia, 19, 552-559.

[45] Zhang, B., Tang, X., Li, Y., Xu, Y., She, W., 2007. Hydrogen production from steam reforming of ethanol and glycerol over ceria-supported metal catalysts. International Journal of Hydrogen Energy, 32, 2367-2373.

[46] Hirai, T., Ikenaga, N.O., Miyake, T., Suzuki, T., 2005. Production of hydrogen by steam reforming of glycerin on ruthenium catalyst. Energy and Fuels, 19, 1761-1762.

[47] Gallegos-Suárez, E. Guerrero-Ruiz, A., Fernández-García, M., Rodríguez-Ramos, I., Kubacka, A., 2015. Efficient and stable Ni–Ce glycerol reforming catalysts: Chemical imaging using X-ray electron and scanning transmission microscopy. Applied Catalysis B: Environmental, 165, 139-148.

[48] Siew, K. W., Lee, H.C., Gimbun, J., Cheng, CK., 2014. Production of CO-rich hydrogen gas from glycerol dry reforming over La-promoted Ni/Al_2O_3 catalyst. International Journal of Hydrogen Energy, 39, 6927-6936.

[49] Dou, B., Wang, C., Song, Y., Chen, H., Xu, Y., 2014. Activity of Ni–Cu–Al based catalyst for renewable hydrogen production from steam reforming of glycerol. Energy Conversion and Management, 78, 253-259.

[50] Chen, C.Y., Lai, W.H., Yan, W.M., Chen, C.C., Hsu, S.W., 2013. Effects of nitrogen and carbon monoxide concentrations on performance of proton exchange membrane fuel cells with Pt–Ru anodic catalyst. Journal of Power Sources, 243, 138-146.

[51] Qi, Z., He, C., Kaufman, A., 2002. Effect of CO in the anode fuel on the performance of PEM fuel cell cathode. Journal of Power Sources, 111(2), 239-247.

[52] Dieuzeide, M.L., Jobbagy, M., Amadeo, N., 2013. Glycerol steam reforming over Ni/γ-Al_2O_3 catalysts, modified with Mg(II). Effect of Mg (II) content. Catalysis Today, 213, 50-57.